Application of Model Based Prognostics to Pneumatic Valves in a Cryogenic Propellant Loading Testbed

Chetan S. Kulkarni *
SGT Inc., NASA Ames Research Center, Moffett Field, CA, 94035

Matthew Daigle †
NASA Ames Research Center, Moffett Field, CA, 94035

George Gorospe ‡
SGT Inc., NASA Ames Research Center, Moffett Field, CA, 94035

Kai Goebel §
NASA Ames Research Center, Moffett Field, CA, 94035

Pneumatic-actuated valves are critical components in many applications, including cryogenic propellant loading for space operations. For these components, failures need to be predicted so that components can be repaired to ensure mission success, i.e., health monitoring and fault prognostics is required. In order to develop, test, mature, and deploy valve prognostics algorithms, we have developed a testbed for pneumatic valves used in cryogenic service for propellant loading operations, in which we can inject controlled damage profiles and observe its effects on valve operation. In this paper, we focus on the prognostics of a continuously-controlled pneumatic valve. We describe the construction of the testbed, the fault injection mechanisms, and the model-based valve prognostics algorithms. Experimental results from the testbed demonstrate successful prediction of valve failure.

I. Introduction

Pneumatic-actuated valves play a critical role in cryogenic propellant loading systems. Since these valves are used to control the flow of propellant, failures may have a significant impact on launch availability.[1] Further, due to the strict safety requirements in such systems, there is a crucial need for valve health monitoring and prognosis. In order to mature this technology, we have constructed a pneumatic valve testbed that allows for the controlled injection of fault degradation profiles with which to test and validate valve prognostics algorithms.[2,3]

In recent work,[4,5] for discretely-operated valves, we developed efficient methods for model-based valve prognostics, requiring only valve opening and closing times (as typically in real operations only valve position is measured) to isolate and identify faults, and to predict end of life (EOL) and remaining useful life (RUL). The approach still follows the general estimation-prediction framework developed in the literature for model-based prognostics.[6,7] In contrast to earlier work on valve prognosis using particle filters,[1,8,9] which can be computationally intensive, the approach in recent work directly maps timing observations to fault parameter values using an offline lookup table computed via simulation using an accurate, medium-fidelity physics-based valve model.

In this work, we follow a similar approach for continuously-operated valves (i.e., valve position can be controlled anywhere between fully closed and fully open). We develop a physics-based model of the valve.

*Research Engineer III, Prognostics Center of Excellence, AIAA Member
†Research Computer Scientist, Prognostics Center of Excellence
‡Research Engineer, Prognostics Center of Excellence
§Technical Area Lead, Discovery and Systems Health, Prognostics Center of Excellence, AIAA Senior Member

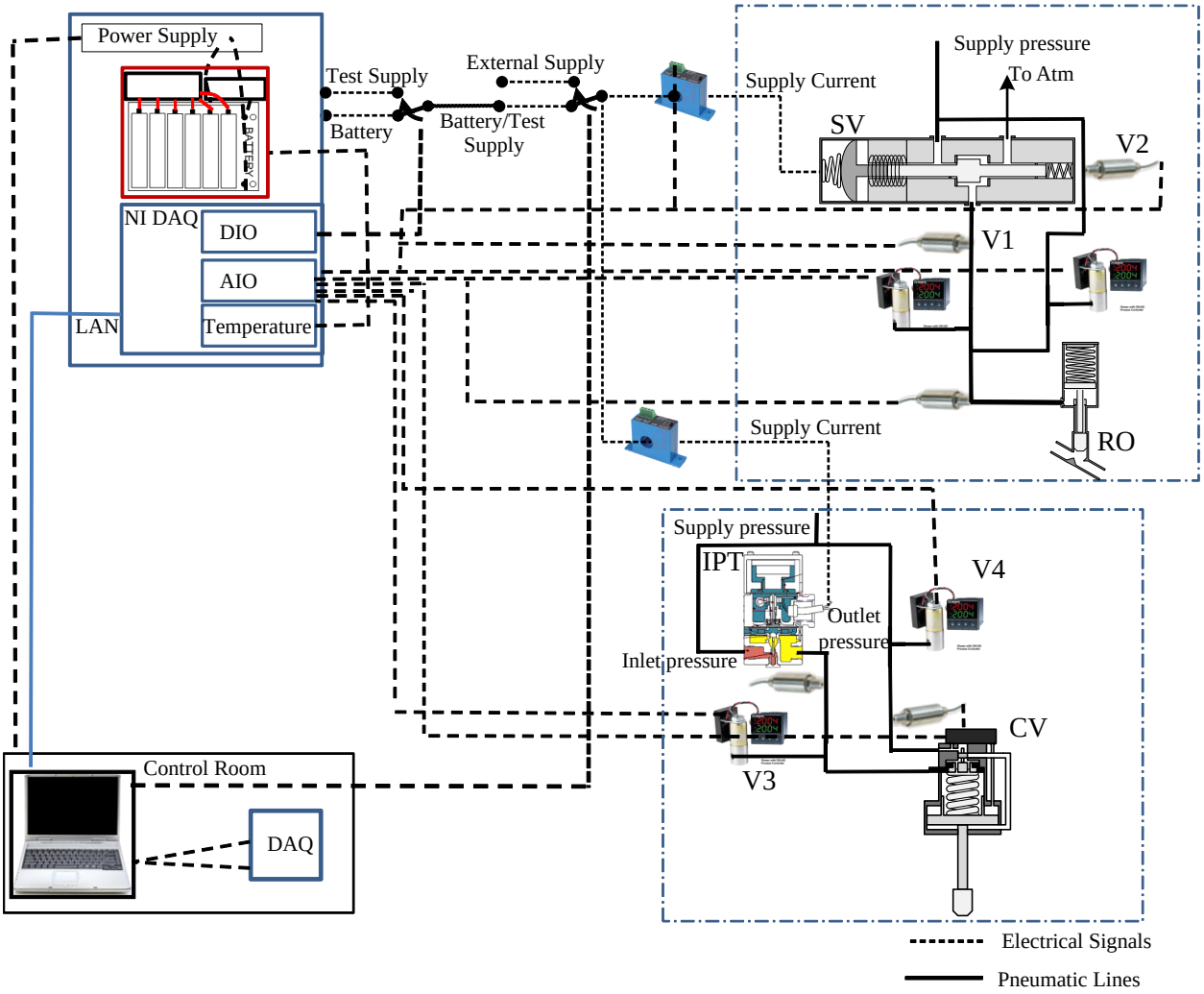

Figure 1. Prognostics demonstration testbed schematic.

We apply a model-based valve prognostics approach and provide experimental results from the testbed demonstrating and validating the approach.

The structure of the paper is as follows. Section II discusses the testbed setup. Section III presents the valve model. Section IV develops the valve prognosis framework, and Section V presents prognosis results using real experimental data from the valve testbed. Section VI concludes the paper.

II. Valve Testbed

The valve prognostics testbed has been developed to demonstrate valve prognosis in the context of cryogenic refueling operations. In this section, we summarize the testbed, highlighting the operation of the continuously-controlled valve on which the technical contributions of this paper are focused. Additional details on the testbed can be found in previous works.[2,3]

The testbed schematic is shown in Fig. 1. The dashed lines denote the electrical signals, including the data acquisition I/O signals, power lines, etc. The solid lines denote the pneumatic pressure lines connecting the supply and the valves. Power is provided by both a typical power supply and a battery backup supply

The testbed includes a continuously-controlled valve (CV), illustrated in Fig. 3 which is a normally-closed valve with a linear cylinder actuator with dual pressure chambers. The valve is positioned by a pressure difference between the primary pressure chamber which is at standard operational pressure and the secondary chamber which can vary in pressure as controlled through the current-pressure transducer (IPT).

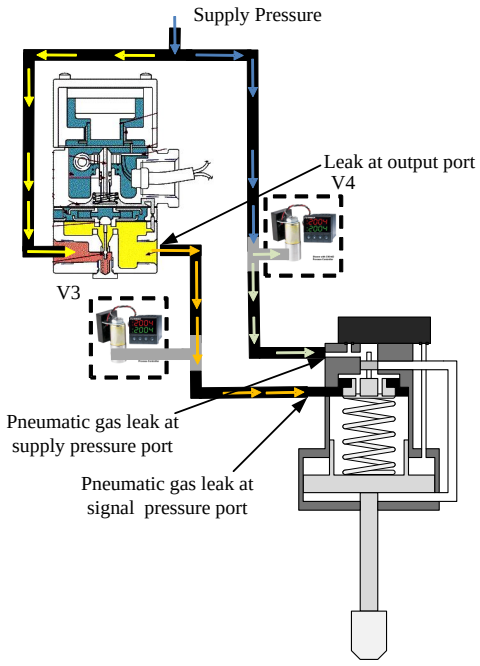

Figure 2. CV valve leaks.

The IPT output pressure is regulated down from the input pressure and is directly proportional to the applied control current supplied to the transducer. Thus, a low current will create a lower output pressure and a higher current will increase the output pressure.

The testbed includes a discrete-controlled valve (DV), which is a normally-open valve with a linear cylinder actuator. The valve is closed by filling the chamber above the piston with gas up to the supply pressure, and opened by evacuating the chamber to atmosphere, with the spring returning the valve to its default position. A three-way two-position solenoid valve (SV), is used for controlling the operation of the DV valve.

With the testbed, we can investigate solenoid valve prognostics,[10] battery prognostics,[11] and pneumatic valve prognostics.[1] In this work, we focus on faults affecting the continuously-operated pneumatic valves (CV). Pneumatic valves can suffer from leaks, increase in friction due to wear, and spring degradation.[1] With the current configuration of the testbed, friction and spring faults cannot be injected or their rate of progression controlled, so we are limited only to leak faults, which, in practice, are the most commonly observed faults. As shown in Fig. 2, two different leak faults for the CV are considered:(i) a leak to atmosphere from the signal line, through valve V3; and (ii) a leak to atmosphere from the supply line, through valve V4. We use the remotely-operated proportional valves V3 and V4 to emulate these leaks. The leak valves allow control over how much they can be opened in order to control the leakage rate and support desired damage progression profiles.

III. Valve Modeling

In order to apply a model-based prognostics approach, we require a dynamic model of the component. To this end, we develop a medium-fidelity physics-based model.

We consider here a normally-closed continuously-controlled valve, shown in Fig. 3. The actuator has two pressure ports, one for the supply pressure, and one for the signal pressure. External to the valve, the signal pressure is controlled between 3–15 psig in order to move the valve between fully closed and fully open. A pressure regulator maintains a loading pressure on top of the valve piston, and the piston moves by modulating the actuating pressure via the pilot valve. The pilot valve, balanced by the spring and the diaphragm assembly, moves up or down according to the signal pressure. When moving up, the volume below the piston is opened up the atmosphere, and when the pilot moves down, the volume below the piston

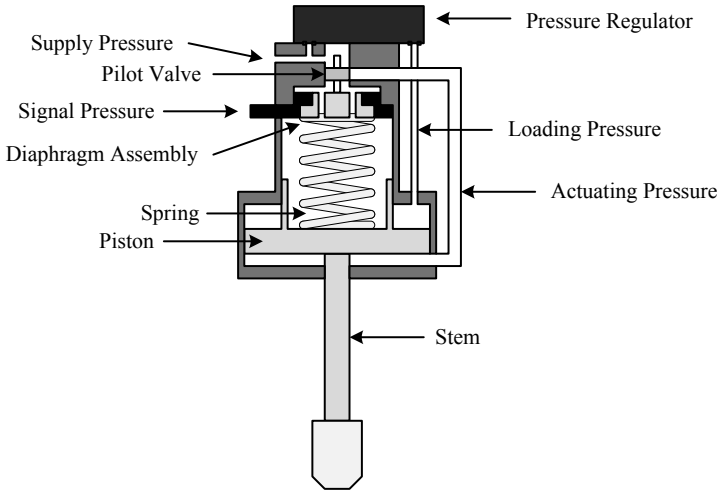

Figure 3. Continuously-controlled valve schematic.

is opened up to the supply pressure.

We present here the model using continuous-time. For implementation purposes, we convert to a discrete-time version using a sample time of 1×10^{-4} s.

We develop a physics model of the valve based on mass and energy balances. The system state includes the position of the piston, $x_p(t)$, velocity of the piston, $v_p(t)$, position of the pilot/spring assembly, $x_s(t)$, velocity of the pilot/spring assembly, $v_s(t)$, mass of gas in volume below the piston $m_b(t)$, mass of gas in the pipe connecting to the supply input, $m_{sp}(t)$, and mass of gas in the pipe connecting to the signal input, $m_{sg}(t)$:

$$\mathbf{x}(t) = \begin{bmatrix} x_p(t) & v_p(t) & x_s(t) & v_s(t) & m_b(t) & m_{sp}(t) & m_{sg}(t) \end{bmatrix}^T. \tag{1}$$

The piston position is defined as $x_p = 0$ when the valve is fully closed, and $x_p = L_s$ when fully open, where L_s is the stroke length of the valve (about 20 mm). When fully closed, the pilot/spring assembly position is also defined as $x_s = 0$.

The derivatives of the states are described by

$$\dot{\mathbf{x}}(t) = \begin{bmatrix} v_p(t) & a_p(t) & v_s(t) & a_s(t) & f_b(t) & f_{sp}(t) & f_{sg}(t) \end{bmatrix}^T, \tag{2}$$

where a is acceleration and f is mass flow.

The two inputs are considered to be

$$\mathbf{u}(t) = \begin{bmatrix} u_{sp}(t) & u_{sg}(t) \end{bmatrix}^T, \tag{3}$$

where $u_{sp}(t)$ is input pressure to the supply port, which is nominally 75 psig, and $u_{sg}(t)$ is the input pressure to the signal port, which varies between 3–15 psig, depending on the commanded valve position.

The acceleration of the piston is defined by the combined mass of the piston and plug, m_p, and the sum of forces acting on the piston, which includes the force from the actuating pressure, $F_a = p_b A_p$, where A_p is the area of the piston in contact with the actuating pressure; the force from the loading pressure, $F_l = A_l p_l$, where A_l is the area of the piston in contact with the loading pressure; friction, $F_f = -r_p v_p(t)$, where r_p is the coefficient of kinetic friction; the spring force, $F_s = k(x_p + x_o - x_s)$ where x_o is the spring compression at the closed position; the weight, $F_w = -m_p g$, and the contact forces, $F_c(t)$, at the boundaries of the valve/piston motion,

$$F_c(t) = \begin{cases} k_c(-x), & \text{if } x < 0, \\ 0, & \text{if } 0 \le x \le L_s, \\ -k_c(x - L_s), & \text{if } x > L_s, \end{cases} \tag{4}$$

where k_c is the (large) spring constant associated with the flexible seals. Overall, the acceleration term is defined by

$$a_p(t) = \frac{1}{m_p}(F_a - F_s - F_l - F_w - F_f + F_c) \tag{5}$$

The pressures p_l is assumed to be constant and known, and the pressure p_b is computed as

$$p_b = \frac{m_b(t)R_gT}{V_{b_0} + A_p x_p(t)}, \tag{6}$$

where we assume an isothermal process in which the (ideal) gas temperature is constant at T, R_g is the gas constant for the pneumatic gas, and V_{b_0} is the minimum gas volume for the gas chamber below the piston.

The acceleration of the pilot/spring assembly is defined by their combined mass, m_s, and the sum of forces acting on the assembly, which includes the force from the spring F_s (as defined above); the force from the signal pressure, $F_{sg} = (p_{sg} - p_{atm})A_d$, where A_d is the area of the diaphragm in contact with the signal pressure and p_{atm} is atmospheric pressure; friction, $F_{fs} = r_s v_s(t)$, where r_s is the coefficient of kinetic friction; the force from the supply pressure, $F_{sp} = (p_{sp} - p_{atm})A_{sp}$, where A_{sp} is the area of the pilot in contact with the supply pressure; the weight, $F_{ws} = m_s g$; and contact forces F_{cs} (defined as above but with L_{ss}, the stroke length of the pilot/spring assembly).

The pressures p_{sg} and p_{sp} are computed as

$$p_{sg} = \frac{m_{sg}(t)R_gT}{V_{sg}}, \tag{7}$$

$$p_{sp} = \frac{m_{sp}(t)R_gT}{V_{sp}}, \tag{8}$$

where V_{sg} is the volume of the pipe containing the signal pressure, and V_{sp} is the volume of the pipe containing the supply pressure.

The mass flows $f_b(t)$, $f_{sp}(t)$, and $f_{sg}(t)$ are defined by

$$f_b(t) = (x_s < 0) \cdot f_g(p_{sp}(t), p_b(t)) - (x_s > 0) \cdot f_g(p_b(t), p_{atm}), \tag{9}$$

$$f_{sp}(t) = f_g(u_{sp}(t), p_{sp}(t)) - f_{sp,leak}(t) - (x_s < 0) \cdot f_g(p_{sp}(t), p_b(t)), \tag{10}$$

$$f_{sg}(t) = f_g(u_{sg}(t), p_{sg}(t)) - f_{sg,leak}(t), \tag{11}$$

where $f_{sg,leak}$ and $f_{sg,leak}$ are leak terms (both leaks to atmosphere). Note also that the flows into and out of the underside of the piston depend on the position of the pilot/spring assembly. Here, f_g defines gas flow through an orifice for choked and non-choked flow conditions.[12] Non-choked flow for $p_1 \geq p_2$ is given by $f_{g,nc}(p_1, p_2) =$

$$C_s A_s p_1 \sqrt{\frac{\gamma}{ZR_gT}\left(\frac{2}{\gamma - 1}\right)\left(\left(\frac{p_2}{p_1}\right)^{\frac{2}{\gamma}} - \left(\frac{p_2}{p_1}\right)^{\frac{\gamma+1}{\gamma}}\right)}, \tag{12}$$

where γ is the ratio of specific heats, Z is the gas compressibility factor, C_s is the flow coefficient, and A_s is the orifice area. Choked flow for $p_1 \geq p_2$ is given by

$$f_{g,c}(p_1, p_2) = C_s A_s p_1 \sqrt{\frac{\gamma}{ZR_gT}\left(\frac{2}{\gamma + 1}\right)^{\frac{\gamma+1}{\gamma-1}}}. \tag{13}$$

Choked flow occurs when the upstream to downstream pressure ratio exceeds $\left(\frac{\gamma+1}{2}\right)^{\gamma/(\gamma-1)}$. The overall gas

flow equation is then given by

$$f_g(p_1,p_2) = \begin{cases} f_{g,nc}(p_1,p_2) & \text{if } p_1 \geq p_2 \\ & \text{and } \frac{p_1}{p_2} < \left(\frac{\gamma+1}{2}\right)^{\frac{\gamma}{(\gamma-1)}}, \\ f_{g,c}(p_1,p_2) & \text{if } p_1 \geq p_2 \\ & \text{and } \frac{p_1}{p_2} \geq \left(\frac{\gamma+1}{2}\right)^{\frac{\gamma}{(\gamma-1)}}, \\ -f_{g,nc}(p_2,p_1) & \text{if } p_2 > p_1 \\ & \text{and } \frac{p_2}{p_1} < \left(\frac{\gamma+1}{2}\right)^{\frac{\gamma}{(\gamma-1)}}, \\ -f_{g,c}(p_2,p_1) & \text{if } p_2 > p_1 \\ & \text{and } \frac{p_2}{p_1} \geq \left(\frac{\gamma+1}{2}\right)^{\frac{\gamma}{(\gamma-1)}}, \end{cases} . \tag{14}$$

The only available measurement is the valve position, so we have

$$\mathbf{y}(t) = \left[x_p(t)\right]. \tag{15}$$

We define end of life through the use of timing limits on the valves, as is done in real valve operations,[1] and also the error in its steady-state position. The valve in the testbed is required to open within 10 s, close within 5 s, and when commanded to open to 100% it must open up at least to 97%.

IV. Valve Prognosis

We describe in this section the prognosis framework developed for the valve. We follow here the same general estimation-prediction framework of model-based prognostics as defined in the scientific literature.[6,7,13] However, since we use only valve timing and steady-state position values for prognosis, we use a simpler estimation approach, based recent work,[4,14] as opposed to more complex and computationally intensive filtering approaches used in previous works.[6,15] We first formulate the prognostics problem, followed by a description of the estimation approach and a description of the prediction approach.

A. Problem Formulation

We assume the system model may be generally defined as

$$\begin{aligned} \mathbf{x}(k+1) &= \mathbf{f}(k, \mathbf{x}(k), \boldsymbol{\theta}(k), \mathbf{u}(k), \mathbf{v}(k)), \\ \mathbf{y}(k) &= \mathbf{h}(k, \mathbf{x}(k), \boldsymbol{\theta}(k), \mathbf{u}(k), \mathbf{n}(k)), \end{aligned}$$

where k is the discrete time variable, $\mathbf{x}(k) \in \mathbb{R}^{n_x}$ is the state vector, $\boldsymbol{\theta}(k) \in \mathbb{R}^{n_\theta}$ is the unknown parameter vector, $\mathbf{u}(k) \in \mathbb{R}^{n_u}$ is the input vector, $\mathbf{v}(k) \in \mathbb{R}^{n_v}$ is the process noise vector, $\mathbf{f}$ is the state equation, $\mathbf{y}(k) \in \mathbb{R}^{n_y}$ is the output vector, $\mathbf{n}(k) \in \mathbb{R}^{n_n}$ is the measurement noise vector, and $\mathbf{h}$ is the output equation.[a]

In prognostics, we are interested in predicting the occurrence of some event E that is defined with respect to the states, parameters, and inputs of the system. We define the event as the earliest instant that some event threshold $T_E : \mathbb{R}^{n_x} \times \mathbb{R}^{n_\theta} \times \mathbb{R}^{n_u} \to \mathbb{B}$, where $\mathbb{B} \triangleq \{0,1\}$ changes from the value 0 to 1.[16] That is, the time of the event k_E at some time of prediction k_P is defined as

$$k_E(k_P) \triangleq \inf\{k \in \mathbb{N} \colon k \geq k_P \wedge T_E(\mathbf{x}(k), \boldsymbol{\theta}(k), \mathbf{u}(k)) = 1\}.$$

The time remaining until that event, Δk_E, is defined as

$$\Delta k_E(k_P) \triangleq k_E(k_P) - k_P.$$

In the context of systems health management, T_E is defined via a set of performance constraints that define what the acceptable states of the system are, based on $\mathbf{x}(k)$, $\boldsymbol{\theta}(k)$, and $\mathbf{u}(k)$.[7] In this context, k_E represents end of life (EOL), and Δk_E represents remaining useful life (RUL). For valves, timing requirements

[a] Bold typeface denotes vectors, and n_a denotes the length of a vector $\mathbf{a}$.

are provided that define the maximum allowable time a valve may take to open or close, and these define T_E.[1] For the CV valve, steady-state position errors are also used to define T_E.

The prognostics problem is to compute estimates of EOL and/or RUL. To do this, we first perform an estimation step that computes estimates of $\mathbf{x}(k)$ and $\boldsymbol{\theta}(k)$, followed by a prediction step that computes EOL/RUL using these values as initial states. For the case of the valve, the future inputs are known, i.e., the valve is simply cycled open and closed, so there is no uncertainty with respect to future inputs.

B. Estimation

Valve position measurements for distance traveled, steady state position and operation time are used for prognostics. We can extract from the continuous position measurement the timing information by computing the difference in time between when the valve is commanded to move, and when it reaches its final position. Using the developed model, we can search for the leak parameter value that matches the observed opening or closing time or steady-state position.

In order to perform the estimation, we construct offline a lookup table, using simulation which maps leak size to open and close times and steady-state position.[4,14] With a fine enough granularity, a lookup table will provide accurate estimates but at a fraction of the computational cost of online estimation methods. To estimate the parameter that defines how the fault evolves in time, we assume a linear progression of the leak parameter and perform a linear regression on the history of estimated leak parameters.

For the signal line leak fault, steady state values are used for fault detection, RUL and EOL estimation. The signal pressure controls the open/close position of the valve while the supply pressure is used for regulating the pressure inside the valve. When this fault is injected, there is no change in the supply pressure but the signal pressure decreases and so the valve is not able to reach its desired steady state final value.

For the supply line leak fault, open time values are used for fault detection, RUL and EOL estimation. When this leak is injected, there is a decrease in the supply pressure, which leads to an increase in the valve opening time (since the corresponding pressure forces take longer to develop). As the leak increases the open time increases accordingly, while the steady state values remain relatively constant.

C. Prediction

Based on the current estimated leak parameter value and regression parameters, we can compute the value of the leak parameter at any future time using the damage progression equation. For the thresholds defined by T_E, we can determine the maximum leak parameter corresponding to EOL, and then using the damage progression equation determine at what future time the leak parameter will reach that value, thus providing EOL.

Both faults have the same qualitative effects; they produce an increase in valve opening time and a decrease in steady-state position. However, their quantitative effects are different; the signal pressure leak has a greater effect on steady-state position and the supply pressure leak a greater effect on opening time. Therefore, we can isolate which fault is present by inspecting which trend is more significant. For a signal leak, the deviation in nominal behavior will be observed first in steady-state position, and for a supply leak, the deviation will be observed first in the opening time. Depending upon the fault isolated the predictions for RUL are computed.

V. Experimental Results

We present here experimental results using the valve prognostics testbed. In each experiment, the valve is cycled open and closed repeatedly, every 10 s, until the EOL condition is reached. The valve under consideration is considered to be failed when it opens in 10 s or greater, closes in 5 s or greater, or the steady state valve percentage when commanded to 100% is 97% or less. In practice, we find that the faults have no significant effect on the valve closing time, so we focus only on opening time and the steady-state position. The nominal valve opening time is around 7.5 s, and we consider a fault detected when open time crosses the 8 s threshold. For the steady-state position, the nominal value (when commanded to 100% open) is 1.005, and we consider a fault detected when it falls below 1.

Faults are injected by linearly increasing the open percentage of the desired leak valve in increments of 1%. We first present results for the signal line leak fault, followed by results for the supply line leak fault.

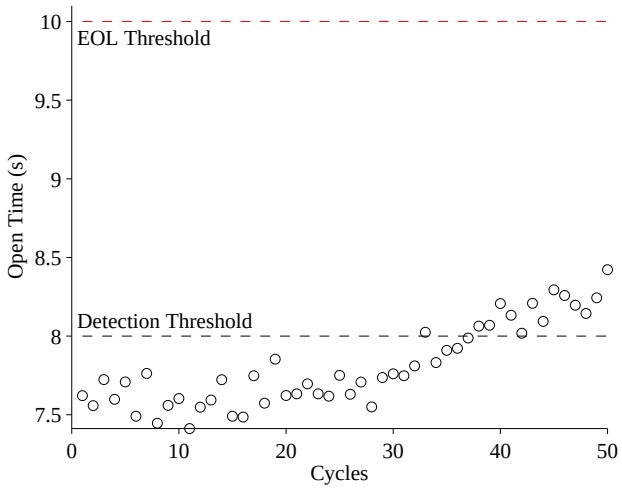

Figure 4. CV Signal Line Leak Fault Open Time

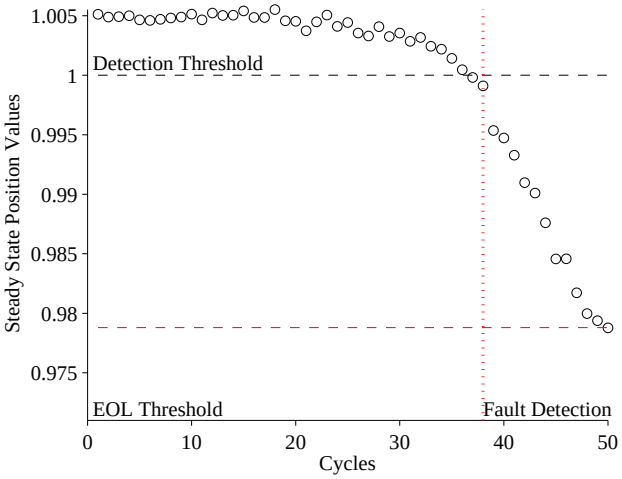

Figure 5. CV Signal Line Leak Fault Steady-State Position

A. Signal Line Leak Fault

As described in Section II, the signal line leak fault is injected by controlling the position of the leak valve V3. This emulates the leak at the output port of the IPT valve or input signal port of the CV. As described in Section III, this fault causes a decrease in the steady state position value and increase in the open times. Fig. 4 shows the open times of the valve during the fault progression which crosses the fault detection threshold but does not cross the EOL threshold, and Fig. 5 shows the steady state values, through which EOL is reached. Both the open times and steady-state position values are noisy hence we take a mean of the last three cycles to determine if either of the values have crossed the detection threshold value. As discussed earlier the leak valve position is increased by 1% every cycle, and by the 38th cycle the steady-state position value crosses the detection threshold. Since the steady-state position detection threshold crossed before the open time threshold, it is determined to be a signal line leak fault which is in agreement with the experiment.

The RUL predictions are given in Fig. 6, where $\alpha = 0.2$ represents a desired accuracy constraint, and RUL^* denotes the true RUL. The predictions converge relatively quickly after the fault is detected, however it is only after the 30th cycle that a noticeable degradation emerges. The algorithm makes predictions which are very close to or within the prediction cone until the end of experiment.

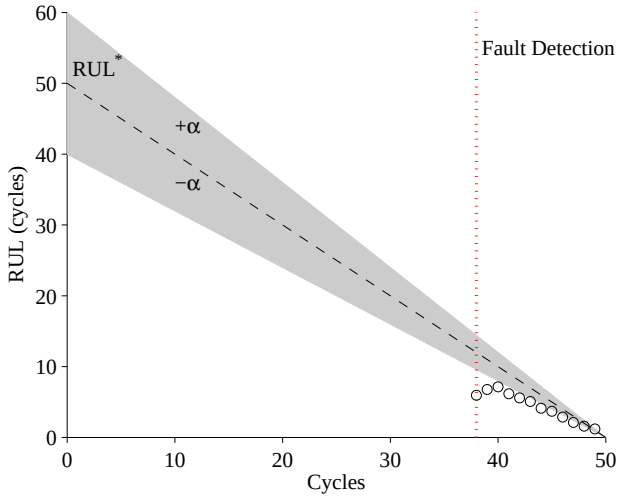

Figure 6. CV Signal Line Leak Fault RUL Predictions

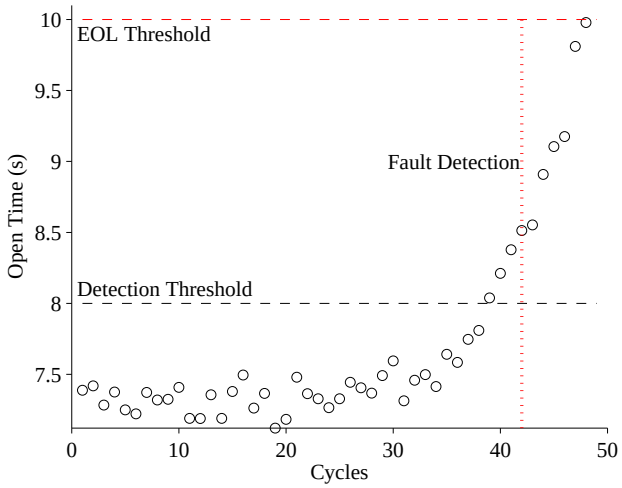

Figure 7. CV Supply Line Leak Fault Open Time

B. Supply Line Leak Fault

As described in Section II, the supply line leak fault is injected by controlling the position of the leak valve V4. As described in Section III, this fault, like the signal line leak fault, causes an increase in opening times and a decrease in steady-state position values. Fig. 7 shows the open times of the valve during the fault progression, and Fig. 8 shows the steady-state position values. Although qualitatively similar, there are large quantitative differences from the observations obtained from the signal line leak fault experiment. A fault is detected at the 43rd cycle based on the opening times, thus a supply line leak fault is correctly diagnosed.

Fig. 9 shows the RUL predictions. After detecting the fault the predictions converge relatively quickly, but, as with the signal line leak fault, a noticeable trend only emerges after 30 cycles. The algorithm makes predictions which are very close to or within the prediction cone until the end of experiment.

VI. Conclusions

In this paper, we described the development of a valve prognostics testbed, focusing on a continuously-controlled valve. We developed a physics model of the valve and a model-based prognostics approach. To demonstrate the approach, we emulated faulty operation by injecting leakage faults in the system. The novel

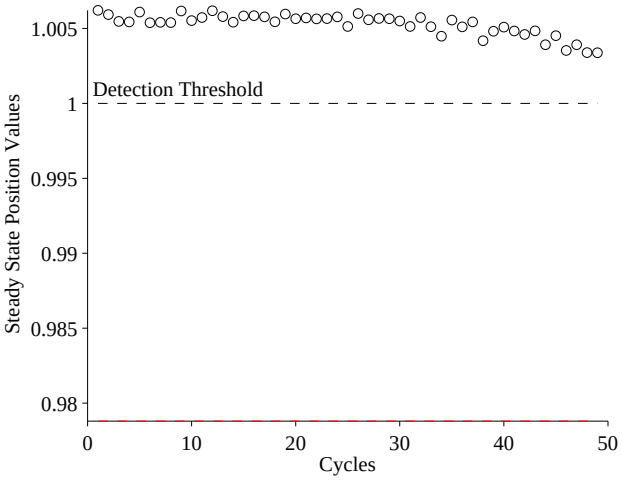

Figure 8. CV Supply Line Leak Fault Steady-State Position

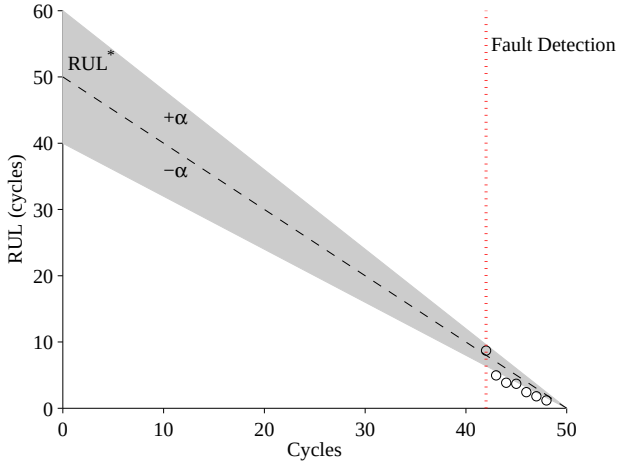

Figure 9. CV Supply Line Leak Fault RUL Predictions

valve prognosis framework operates with limited measurements, using only valve timing and steady state position information, but was demonstrated to provide accurate EOL predictions.

Future work will involve conducting more testbed experiments to improve the developed model and prognosis framework, and further validate the algorithms with experimental data from the testbed.

Acknowledgment

This work was funded in part by the NASA System-wide Safety Assurance Technologies (SSAT) project under the Aviation Safety (AvSafe) Program of the Aeronautics Research Mission Directorate (ARMD), by the NASA Automated Cryogenic Loading Operations (ACLO) project under the Office of the Chief Technologist (OCT) of Advanced Exploration Systems (AES), and by the Advanced Ground Systems Maintenance (AGSM) Project under the Ground Systems Development and Operations program.

References

[1]Daigle, M. and Goebel, K., "A Model-based Prognostics Approach Applied to Pneumatic Valves," *International Journal of Prognostics and Health Management*, Vol. 2, No. 2, Aug. 2011.

[2]Kulkarni, C., Daigle, M., and Goebel, K., "Implementation of Prognostic Methodologies to Cryogenic Propellant Loading

Testbed," *IEEE AUTOTESTCON 2013*, Sept. 2013.

[3]Kulkarni, C., Gorospe, G., Daigle, M., and Goebel, K., "A Testbed for Implementing Prognostic Methodologies on Cryogenic Propellant Loading Systems," *IEEE AUTOTEST 2014*, September 2014.

[4]Daigle, M., Kulkarni, C., and Gorospe, G., "Application of Model-based Prognostics to a Pneumatic Valves Testbed," *2014 IEEE Aerospace Conference*, March 2014.

[5]Kulkarni, C., Daigle, M., Gorospe, G., and Goebel, K., "Validation of Model-Based Prognostics for Pneumatic Valves in a Demonstration Testbed," *Annual Conference of the Prognostics and Health Management Society 2014*, September 2014, pp. 76–85.

[6]Orchard, M. and Vachtsevanos, G., "A Particle Filtering Approach for On-Line Fault Diagnosis and Failure Prognosis," *Transactions of the Institute of Measurement and Control*, Vol. 31, No. 3-4, June 2009, pp. 221–246.

[7]Daigle, M. and Goebel, K., "Model-based Prognostics with Concurrent Damage Progression Processes," *IEEE Transactions on Systems, Man, and Cybernetics: Systems*, Vol. 43, No. 4, May 2013, pp. 535–546.

[8]Daigle, M. and Goebel, K., "Prognostics for Ground Support Systems: Case Study on Pneumatic Valves," *Proceedings of AIAA Infotech@Aerospace 2011 Conference*, March 2011.

[9]Daigle, M. and Goebel, K., "Model-based prognostics under limited sensing," *2010 IEEE Aerospace Conference*, March 2010.

[10]Daigle, M. and Goebel, K., "Improving computational efficiency of prediction in model-based prognostics using the unscented transform," *Proc. of the Annual Conference of the Prognostics and Health Management Society 2010*, Oct. 2010.

[11]Daigle, M. and Kulkarni, C., "Electrochemistry-based Battery Modeling for Prognostics," *Annual Conference of the Prognostics and Health Management Society 2013*, Oct. 2013, pp. 249–261.

[12]Perry, R. and Green, D., *Perry's chemical engineers' handbook*, McGraw-Hill Professional, 2007.

[13]Luo, J., Pattipati, K. R., Qiao, L., and Chigusa, S., "Model-based prognostic techniques applied to a suspension system," *IEEE Transactions on Systems, Man and Cybernetics, Part A: Systems and Humans*, Vol. 38, No. 5, Sept. 2008, pp. 1156 –1168.

[14]Teubert, C. and Daigle, M., "I/P Transducer Application of Model-Based Wear Detection and Estimation using Steady State Conditions," *Proceedings of the Annual Conference of the Prognostics and Health Management Society 2013*, Oct. 2013, pp. 134–140.

[15]Daigle, M., Saha, B., and Goebel, K., "A Comparison of Filter-based Approaches for Model-based Prognostics," *2012 IEEE Aerospace Conference*, March 2012.

[16]Daigle, M. and Sankararaman, S., "Advanced Methods for Determining Prediction Uncertainty in Model-Based Prognostics with Application to Planetary Rovers," *Annual Conference of the Prognostics and Health Management Society 2013*, Oct. 2013, pp. 262–274.